Molecular Biology of the Cell
Vol. 6, 1535–1547, November 1995

Identification of the Sequences in HMG-CoA Reductase Required for Karmellae Assembly

Mark L. Parrish,* Christian Sengstag,† Jasper D. Rine,‡ and Robin L. Wright*§

*Department of Zoology, University of Washington, Seattle, Washington 98195; †Institut für Toxikologie, der Eidgenössischen Technischen Hochschule, ünd der Universitat Zürich, CH-8603 Schwerzenbach, Switzerland; and ‡Division of Genetics, Department of Molecular and Cellular Biology, University of California, Berkeley, California 94720

Submitted June 19, 1995; Accepted August 16, 1995
Monitoring Editor: Keith R. Yamamoto

In all eukaryotic cells that have been examined, specific membrane arrays are induced in response to increased levels of the ER membrane protein, HMG-CoA reductase. Analysis of these inducible membranes has the potential to reveal basic insights into general membrane assembly. Yeast express two HMG-CoA reductase isozymes, and each isozyme induces a morphologically distinct proliferation of the endoplasmic reticulum. The isozyme encoded by *HMG1* induces karmellae, which are long stacks of membranes that partially enclose the nucleus. In contrast, the isozyme encoded by *HMG2* induces short stacks of membrane that may be associated with the nucleus, but are frequently present at the cell periphery. To understand the molecular nature of the different cellular responses to Hmg1p and Hmg2p, we mapped the region of Hmg1p that is needed for karmellae assembly. For this analysis, a series of exchange alleles was examined in which a portion of the Hmg2p membrane domain was replaced with the corresponding Hmg1p sequences. Results of this analysis indicated that the ER lumenal loop between predicted transmembrane domains 6 and 7 was both necessary and sufficient for karmellae assembly, when present in the context of an HMG-CoA reductase membrane domain. Immunoblotting experiments ruled out the simple possibility that differences in the amounts of the various chimeric HMG-CoA reductase proteins was responsible for the altered cellular responses. Our results are consistent with the hypothesis that each yeast isozyme induces or organizes a qualitatively different organization of ER membrane.

INTRODUCTION

Assembly of specific membranes is an essential process throughout cell growth and development. Nevertheless, the mechanisms by which cells achieve this specificity are not understood in even a single case. A useful approach to unravel these mechanisms focuses on the specific membrane biogenesis induced by a subset of membrane proteins (Chin *et al.*, 1982; Von Meyenburg *et al.*, 1984; Weiner *et al.*, 1984; Elmes *et al.*, 1986; Wright *et al.*, 1988). One of the best characterized of these proteins is HMG-CoA reductase, an integral ER membrane protein that catalyzes the rate-limiting step in cholesterol biosynthesis (see Goldstein and Brown, 1990 for recent review). In all organisms that have been tested, elevations in the level of HMG-CoA reductase lead to the assembly of cell type–specific membrane arrays (Chin *et al.*, 1982; Anderson *et al.*, 1983; Pathak *et al.*, 1986; Li *et al.*, 1988; Singer *et al.*, 1988; Wright *et al.*, 1988; Andreis *et al.*, 1990; Wright *et al.*, 1990). For example, mammalian cells assemble hexagonal arrays of smooth membrane tubules known as crystalloid ER (endoplasmic reticulum) (Chin *et al.*, 1982; Anderson *et al.*, 1983; Pathak *et al.*, 1986). In contrast, yeast cells assemble stacked membrane arrays (Wright *et al.*, 1988; Koning and Wright, unpublished data).

§ Corresponding author.

In animals and fungi, HMG-CoA reductase is bound to membranes via a complex membrane domain that spans the bilayer at least seven times (Liscum *et al.*, 1985; Olender and Simoni, 1992; Roitelman *et al.*, 1992). Although this domain has no role in the catalytic activity of HMG-CoA reductase, it is essential for both sterol-induced degradation of HMG-CoA reductase (Chin *et al.*, 1985; Gil *et al.*, 1985; Skalnik *et al.*, 1988) and for induction of membrane biogenesis (Jingami *et al.*, 1987; this study). One model to account for HMG-CoA reductase-induced membrane biogenesis is that the membrane-bound domain of the protein delivers a signal for production of specific membrane arrays. Cells respond to this signal by producing the necessary proteins and lipids that are assembled with HMG-CoA reductase into the membrane array. The nature of the putative signal is unknown, but may require specific sequences in the membrane domain.

Consistent with this model, the specific organization of the membranes formed in response to HMG-CoA reductase is cell-type specific (Wright *et al.*, 1990). For example, although the amino acid sequences of the membrane domains of mammalian and yeast HMG-CoA reductase have no sequence homology, each is capable of inducing membranes in the other cell type. However, the membranes formed are determined by the cell type in which the membranes are assembled. Consequently, expression of mammalian HMG-CoA reductase in yeast leads to karmellae, rather than crystalloid ER formation. In contrast, expression of yeast HMG-CoA reductase in mammalian cells leads to crystalloid ER, rather than karmellae assembly. These results suggest that cell-specific factors are involved in organization of the amplified membranes.

Unlike mammalian cells that have only a single HMG-CoA reductase gene, yeast carry a pair of genes, *HMG1* and *HMG2*, that each encodes a functional HMG-CoA reductase isozyme (Basson *et al.*, 1986). *HMG1* and *HMG2* encode proteins (referred to as Hmg1p and Hmg2p) with nearly identical catalytic domains and either gene can support cell viability (Basson *et al.*, 1986). Less homology is present in the membrane domain sequence, although the secondary structures of the membrane domains are similar, if not identical (Basson *et al.*, 1986; Sengstag *et al.*, 1990). Interestingly, each isozyme induces a morphologically distinct organization of stacked membranes (Wright *et al.*, 1988; Koning and Wright, unpublished observations). Cells that express 10-fold elevated levels of Hmg1p assemble karmellae, which are long stacks of membranes that partially encircle the nucleus. In contrast, cells that express 10-fold elevated levels of Hmg2p assemble short stacks of membranes that can be near the nucleus, but are frequently at the cell periphery. Thus, although they are functionally interchangeable and structurally similar, each yeast HMG-CoA reductase isozyme produces a different and readily observable cellular response.

As a first step in understanding the mechanics and regulation of specialized membrane biogenesis, the different cellular responses to Hmg1p and Hmg2p were exploited to map the karmellae-inducing sequences in Hmg1p. Specifically, we examined cells expressing chimeric proteins that replaced portions of the Hmg1p membrane domain with the corresponding Hmg2p sequences. As expected from similar studies in mammalian cells, the activity of HMG-CoA reductase was not required for stimulation of membrane proliferation. In addition, results of this analysis demonstrated that a region of the Hmg1p predicted to lie in the ER lumen was both necessary and sufficient to induce karmellae assembly. Quantitative differences in amounts of the chimeric proteins could not account for the altered membrane assembly. Thus, these results raise the possibility that the signal for karmellae assembly may operate through protein-protein interactions that occur in the ER lumen.

MATERIALS AND METHODS

Strains and Media

The yeast strains used in this study are listed in Table 1. Strains containing plasmids were grown at 30°C on modified minimal medium (0.67% yeast nitrogen base without amino acids, 2% glucose, 2% casamino acids) supplemented with the appropriate amino acids or nucleotide bases (Sherman *et al.*, 1986). Strains not containing plasmids were grown on YPD (2% yeast extract, 2% Bactopeptone, and 2% glucose) (Sherman *et al.*, 1986). Solid medium contained 2% agar. Membrane morphology was assayed on cultures at OD_{600} of 0.5 or less (early logarithmic phase)

Molecular Genetic Manipulations

Construction of the genes that encode Hmg1:Hmg2 fusion proteins is described by Sengstag *et al.* (1990). In brief, the fusion proteins consist of the membrane domain of HMG-CoA reductase (amino-terminal 525 amino acids), followed by the first 307 amino acids of mature invertase, and terminated with the carboxyl-terminal 767 amino acids of histidinol dehydrogenase. To produce the different members of this fusion protein series, sequences encoding increasing portions of the Hmg1p membrane domain were systematically replaced with the corresponding Hmg2p sequences. The junctions between Hmg1p and Hmg2p sequences in all of the fusions occur at the carboxyl terminus of a predicted transmembrane domain. The resulting series of fusion proteins have progressively increasing proportions of the Hmg2p membrane domain, such that the Hmg2p sequences are present at the amino terminus and terminate at a predicted transmembrane domain. In this report, these proteins are referred to as $Hmg1_{(1-7)}$:Suc2:His4p, $Hmg2_{(1)}$:$Hmg1_{(2-7)}$:Suc2:His4p, and so forth. The numbers in parentheses after "Hmg1" and "Hmg2" refer to the transmembrane domains from the particular isozyme that are present in the fusion protein. Thus, $Hmg2_{(1)}$:$Hmg1_{(2-7)}$:Suc2:His4p contains the first transmembrane domain from Hmg2p and the second through seventh transmembrane domains from Hmg1p (see Table 1).

To exchange Hmg1p and Hmg2p "Loop G" sequences (the region between transmembrane domains 6 and 7), site-directed mutagenesis was used to introduce in-frame *Sal*I and *Xho*I sites flanking the Loop G-encoding sequences (Altered Sites, Promega, Madison, WI). For Hmg1p, an *Xho*I site was placed at the 5′ end and a *Sal*I site was

placed at the 3′ end of the Loop G sequence. For Hmg2p, a *Sal*I site was placed at the 5′ end and an *Xho*I site was placed at the 3′ end of the Loop G sequences. The regions encoding Loop G were exchanged in two steps, taking advantage of the complementarity of *Xho*I and *Sal*I restriction fragments. To fuse the altered Hmg1p membrane domain together with carboxyl terminal Suc2:His4p sequences, the 2.4-kb *Eco*RI fragment containing the promoter and membrane domain coding sequences of $Hmg1_{(Hmg2\ Loop\ G)}$ was blunted, using the Klenow fragment of DNA polymerase, and ligated into the *Sma*I site of pCS3, producing pRW377. This plasmid was transformed into JRY396, yielding RWY591, which produced $Hmg1_{(Hmg2\ Loop\ G)}$:Suc2:His4p. To fuse the altered Hmg2p membrane domain with the Hmg2p carboxyl sequences, the 3-kb *Sac*I–*Bam*HI fragment containing the promoter and membrane domain coding sequences of $Hmg2_{(Hmg1\ Loop\ G)}$ was ligated into a modified pJR360 in which the *Bam*HI site in the polylinker was destroyed by filling in with the Klenow fragment of DNA polymerase and religating. This plasmid, pMP375, was transformed into JRY396 producing RWY589, which expresses $Hmg2_{(Hmg1\ Loop\ G)}$.

Light Microscopy

Early log-phase cells (OD_{600} = 0.3–0.5) were stained with 10 μg/ml $DiOC_6$ (Kodak, Rochester, NY) per 10^7 cells and the cells were examined using fluorescein filter combinations (Excitation 480 ± 20 nm, Barrier 535 ± 40 nm) on a Nikon Microphot-FXA fluorescence microscope (Koning *et al.*, 1993). Photographs of $DiOC_6$-stained cells were taken using Polaroid type 57 film (3000 ASA). Alternately, the stained cells were observed with laser scanning confocal microscopy using a Bio-Rad MRC6000 laser scanning confocal microscope (488-nm excitation wavelength and BHS emission filter; Richmond, CA).

The immunofluorescence procedure was modified from methods described by Pringle *et al.* (1989). Specifically, 3–5 ml of an early log-phase culture (0.3–0.5 OD_{600} per ml) was fixed for 2 h in 3.7% formaldehyde. Cells were washed twice by centrifugation and resuspension in 1.2 M sorbitol, 100 mM potassium phosphate, pH 7.5. For partial removal of the cell wall, the washed cell pellet was resuspended in 0.5 ml of this buffer to which had been added 1 μl of β-mercaptoethanol, 10 μl glusulase (Sigma Chemicals, St. Louis, MO), and 50 μl of 1 mg/ml zymolyase 20T (ICN, Irvine, CA). After incubation at 37°C for 15 min, the cells were washed twice by centrifugation and resuspension in Tris-buffered saline (TBS). A 15-μl aliquot of the washed cell suspension was applied to each well of a multiwell slide (Cell-line Associates, Newfield, NJ), which had previously been treated for 15 min with 1% aqueous polyethylenimine, then rinsed in tap water, and air dried. The cells were allowed to settle and adhere during a 15-min incubation in a moist chamber; then the nonadherent cells were removed by aspiration and the

Table 1. Yeast strains used in this study

Strain number	Description	Notes
JRY396[a]	MATa leu2-3 leu2-112	host strain
(alias RSY198)	prc1::LEU2 suc2D9 ura3-52	invertase and carboxypeptidase Y deficient
JRY282[a]	JRY396 + pA (multicopy YEp352 vector)	produces Hmg1:Suc2:His4 fusion
JRY283[a]	JRY396 + pX1,6 (multicopy YEp352 vector)	produces $Hmg2_{(1)}$:$Hmg1_{(2-7)}$: Suc2:His4p fusion
JRY284[a]	JRY396 + pX2,5 (multicopy YEp352 vector)	produces $Hmg2_{(1-2)}$:$Hmg1_{(3-7)}$: Suc2:His4p fusion
JRY285[a]	JRY396 + pX3,4 (multicopy YEp352 vector)	produces $Hmg2_{(1-3)}$:$Hmg1_{(4-7)}$: Suc2:His4p fusion
JRY286[a]	JRY396 + pX4,3 (multicopy YEp352 vector)	produces $Hmg2_{(1-4)}$:$Hmg1_{(5-7)}$: Suc2:His4p fusion
JRY287[a]	JRY396 + pX5,2 (multicopy YEp352 vector)	produces $Hmg2_{(1-5)}$:$Hmg1_{(6-7)}$: Suc2:His4p fusion
JRY288[a]	JRY396 + pX6,1 (multicopy YEp352 vector)	produces $Hmg2_{(1-6)}$:$Hmg1_{(7)}$: Suc2:His4p fusion
JRY289[a]	JRY396 + pX7,0 (multicopy YEp352 vector)	produces Hmg2:Suc2:His4p fusion
JRY290[a]	JRY396 + pAD7 (multicopy YEp352 vector)	produces $Hmg1_{(1-6)}$:Suc2:His4p fusion
RWY249[b]	JRY396 + YEpHmg2 (multicopy YEp352 vector)	expresses native Hmg2p
RWY605 this work	JRY396 + pJR360 (multicopy pSEY 8 vector)	expresses native Hmg2p
RWY589 this work	JRY396 + pMP375 (multicopy pSEY 8 vector)	expresses $Hmg2_{(Hmg1\ "Loop\ G")}$ protein
RWY591 this work	JRY396 + pRW377 (multicopy pSEY 8 vector)	expresses $Hmg1_{(Hmg2\ "Loop\ G")}$: Suc2:His4p fusion protein
JRY384[a]	JRY396 + YEp352 (multicopy vector)	control strain contains vector only
JRY383[b]	JRY396 + pJR59 (multicopy YEp24 vector)	expresses native Hmg1p

[a] Sengstag, *et al.*, 1990.

[b] Rine, *et al.*, 1983.

[c] Basson, *et al.*, 1988.

wells were washed three to five times with 30-μl droplets of TBS. A 10-μl droplet of blocking solution, TBSTO (2% ovalbumin, 0.05% Tween-20 in TBS), was applied and allowed to incubate at room temperature for 15 min. An equal volume of antisera diluted in TBSTO was added and incubated for 1–2 h. Following washing (five times by aspiration and application of 30-μl droplets of TBS), fluorescein-labeled goat anti-rabbit antiserum (Cappel/Organon Technica, Durham, NC) diluted 1:2000 in TBSTO was added and allowed to bind for 1 h at room temperature. The wells were washed as before and then a 20-μl droplet of 1 μg/ml 4,6,-diamidino-2-phenylindole in TBS was added. Following incubation for 5 min, the wells were washed twice with TBS, 5 μl of Citifluor mounting solution (Ted Pella, Redding, CA) was applied to each well, and a coverslip was added and sealed in place with nail polish. A polyclonal antiserum against α-tubulin, provided by Frank Solomon (Massachusetts Institute of Technology, Cambridge, MA), was used as a positive control for the staining procedure. Affinity-purified anti-invertase antiserum was provided by Randy Schekman (University of California, Berkeley, CA). Antiserum against Kar2p was a gift from Dr. Jeff Brodsky (University of Pittsburgh, Pittsburgh, PA). The fluorescence intensity observed with the anti-invertase antiserum was too low for conventional photography. Consequently, the signal was captured and amplified using a silicon-intensified video camera and analysis system (DAGE-MTI, Michigan City, IN). Hard-copy images from the video display were made using a video printer (Seikosha, Mahwah, NJ).

PAGE and Immunoblotting

Crude membrane fractions were prepared from logarithmic phase cultures using modifications of a method described by Deschenes and Broach (1987). Cultures were harvested and resuspended in lysis buffer (0.3 M sorbitol, 0.1 M NaCl, 5 mM $MgCl_2$, and 10 mM Tris-HCl, pH 7.4) containing 1 μg/ml TPCK, leupeptin, pepstatin A, and 1 mM PefaBloc SC (Boehringer Mannheim Biochemica, Indianapolis, IN). Acid-washed glass beads were added to the meniscus and the sample was agitated for 1 min in a Mini-Beadbeater (Biospec, Bartlesville, OK). The lysate was removed from the beads and cleared by several 4-s spins in a microcentrifuge. (A small amount of cross-reactive material was present in this pellet). Membranes were pelleted by centrifugation for 20 min at top speed in a microcentrifuge, resuspended in lysis buffer, and repelleted. The final pellet was resuspended in 10 μl of lysis buffer per 10^7 cells and divided into aliquots before storing at −75°C. For SDS-PAGE, an equal volume of 2 × sample buffer (8 M urea, 4% SDS, 10% β-mercaptoethanol, 20% glycerol, 0.125 M Tris-HCl, pH 6.8) was added, and the sample was heated for 15 min at 55–60°C. The proteins were separated on 7.5% or 10% polyacrylamide minigels, using a 3% stacking gel that contained 8 M urea. Following electrophoresis, the proteins were transferred to nitrocellulose in a semi-dry transfer apparatus (Hoefer, San Francisco, CA) operated at 100 mA for 1 h. After blocking overnight in TBSTM (2% nonfat dry milk, 0.05% Tween-20 in TBS), the blot was incubated for 2 h in anti-invertase antiserum diluted 1:10,000 in TBSTM or anti-Hmg2p diluted 1:500 in TBSTM (the antisera was produced against the C-terminal 15 amino acids of Hmg2p: QPSNKGPPCKTSALL). Following three washes in TBSTM, the blot was incubated for 1 h in alkaline phosphatase–conjugated goat anti-rabbit antiserum (Promega, Madison, WI) diluted 1:7500 in TBSTM. The blot was then washed three times in TBSTM, twice in TBST and twice in TBS, and then developed using 10 μg/ml nitroblue tetrazolium and 5 μg/ml 5-bromo-4-choro-3-indolyl phosphate in 0.1 M Tris-HCl, pH 9.5, 0.1 mM NaCl, 5 mM $MgCl_2$ as substrates. Dried gels and immunoblots were digitized using a Scan-X Color Scanner (HSD Microcomputer, Mountain View, CA). Relative amounts of total protein loaded per lane as well as relative amounts of Hmg1p or Hmg2p on the immunoblots were determined using the NIH Image 1.54 Analysis software. Serial dilutions of samples were loaded and analyzed to evaluate whether the immunoblots were in the linear range of the alkaline phosphatase reaction.

RESULTS

Experimental Strategy

To map the karmellae-inducing region of Hmg1p, we examined cells expressing a series of recombinant forms of HMG-CoA reductase in which increasing amounts of the Hmg1p membrane domain were replaced with the corresponding Hmg2p sequences. All fusion genes were present on multi-copy plasmids that were present in approximately 10 copies per cell. Thus, the increased gene dosage led to concomitant increases in the amount of the HMG-CoA reductase membrane domain encoded by the particular plasmid carried by the cell. The fusion gene containing the entire Hmg1p membrane domain was expressed from the *HMG1* promoter. However, the other fusion genes in this series were expressed from the *HMG2* promoter. With one exception, the HMG-CoA reductase carboxyl terminus, which contains the catalytic domain, was replaced with sequences from Suc2p and His4p (Sengstag *et al.*, 1990). The Suc2p sequences served as an immunological tag and the His4p sequences encoded histidinol dehydrogenase, an activity that is functional only when in the cytoplasm (DeShaies and Schekman, 1987). This Suc2p-His4p carboxyl terminus was useful for in vivo and in vitro tests of yeast HMG-CoA reductase topology (Sengstag *et al.*, 1990).

The ability of the fusion proteins to induce karmellae was determined by staining living cells with the lipophilic fluorescent dye $DiOC_6$. Under the conditions used in this study, $DiOC_6$ specifically stained the nuclear envelope and endoplasmic reticulum, allowing the presence of membrane proliferations to be rapidly assessed and quantitated (Koning *et al.*, 1993). Cells that lacked karmellae were distinguished by dim, uniform nuclear envelope staining (Figure 1A). In contrast, cells with karmellae membrane proliferations were characterized by bright, asymmetric nuclear envelope staining (Figure 1, B–D).

Identification of the Sequences in the Hmg1p Membrane Domain Required for Karmellae Assembly

Cells expressing either intact Hmg1p (JRY383) or the fusion protein containing the entire Hmg1p membrane domain fused to Suc2:His4p (JRY282) possessed karmellae (summarized in Figure 2). This result confirmed that, as observed in mammalian cells, the sequences required for membrane induction were present in the membrane domain. Thus, elevations of HMG-CoA reductase activity were not required for induction of membrane biogenesis. Rather, the membrane-associated region was sufficient for karmellae induction. Karmellae were observed in 20% of the cells expressing the intact Hmg1p protein (Figure 3A) and

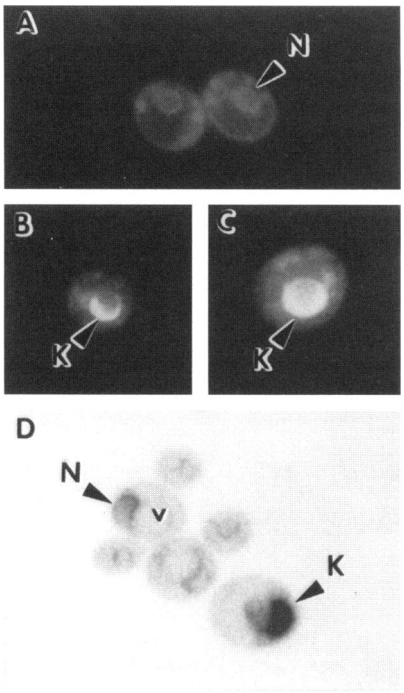

Figure 1. $DiOC_6$-staining rapidly revealed the presence and distribution of karmellae membranes in yeast cell populations. (A) $DiOC_6$ staining patterns of a vector-containing control strain that did not assemble karmellae (JRY384). Nuclei that lacked karmellae were readily distinguished by the uniform intensity of nuclear envelope staining. Cells with this staining pattern were scored as karmellae minus. However, it is possible that the staining was not sufficiently sensitive to visualize nuclei with only one or two karmellae layers. Consequently, $DiOC_6$ staining may underestimate the number of cells in a population that possesses karmellae. In addition, karmellae were scored as present in approximately 1% of the cells observed from staining, but not overproducing HMG-CoA reductase. These observations presumably reflect the intrinsic error rate in scoring. All experiments were conducted in a manner in which the person scoring the karmellae frequency was unaware of strain identity. (B and C) $DiOC_6$ staining patterns of a strain that overproduced Hmg1p revealed that karmellae were present in 32% of the population (JRY282). Karmellae-containing nuclei had distinctly asymmetric staining of the nuclear envelope. (D) A reverse image of JRY282 stained with $DiOC_6$. A prominent karmellae-containing nucleus is present in the lower right of the image (marked with the arrowhead and the letter K). The other arrow (with the letter N) points to a nucleus that contained much less prominent karmellae. Karmellae are not visible in the other four cells. Fluorescence microscopy, 1200×.

in 32% of cells expressing the $Hmg1_{(1-7)}$:Suc2:His4p fusion protein (Figure 3B). Because karmellae are retained within the mother cell at mitosis, karmellae are expected to be in at most 50% of cells in a log phase culture. A key issue is how well the $DiOC_6$ staining reported the presence of karmellae. Based on electron microscopy, karmellae membranes are present in 35% of log-phase cells expressing intact Hmg1p (Wright and Rine, 1989). The frequency of karmellae observed by $DiOC_6$ staining in strains expressing the $Hmg1_{(1-7)}$:Suc2:His4p fusion protein was near this expected value of 35%; however, as judged by $DiOC_6$ staining, the frequency of membrane proliferations was lower than expected in strains expressing the intact Hmg1p protein. This lower frequency may reflect limitations of the $DiOC_6$ staining procedure. If so, the frequencies reported in Figure 2 under-represented the presence of karmellae. Nevertheless, karmellae were both more frequently observed and more prominent in cells expressing the $Hmg1_{(1-7)}$:Suc2:His4p fusion protein than in those expressing the intact Hmg1p protein.

We examined the complete series of fusion proteins in which increasing portions of Hmg1p were replaced with the corresponding Hmg2p sequences. All proteins that contained at least the last loop and transmembrane domain of Hmg1p (i.e., Loop G and TMD7) were able to induce karmellae formation (Figure 2 and Figure 3, C–H). Thus, karmellae membranes were assembled in cells that expressed fusion proteins containing this portion of Hmg1p, even when the remainder of the membrane domain consisted of Hmg2p sequences (see Figure 4). In contrast, only 3% of the cells expressing the fusion protein that contained the entire Hmg2p membrane domain assembled karmellae. Although short stacks of membranes are present at the cell periphery and near the nucleus of cells expressing Hmg2p (Koning and Wright, unpublished observations), karmellae are not observed by electron microscopy or $DiOC_6$ staining in cells expressing wild-type Hmg2p. Thus, even the small number of karmellae observed in the strain expressing $Hmg2_{(1-7)}$:Suc2:His4p strain was unexpected.

A straightforward interpretation of these results was that information needed to generate karmellae was not present in the first six transmembrane domains of Hmg1p nor in the loops that link these transmembrane domains. In addition, these results suggested that a karmellae-inducing signal was present in the carboxyl-terminal portion of the Hmg1p membrane domain, perhaps extending from Loop G through transmembrane domain 7 (Figure 4). Consistent with this possibility, a fusion that placed the Suc2:His4p domain in the center of Loop G, thus deleting transmembrane domain 7 and a large portion of Loop G, did not induce karmellae assembly ($Hmg1_{(1-6)}$:Suc2:His4p, Figure 2).

Differences in the Steady-state Amounts of Fusion Proteins Did Not Account for Differences in Karmellae-inducing Ability

In principle, quantitative differences in the amount of fusion proteins accumulated by the cells might underlie at least some of the differences in karmellae biogenesis. If so, the chimeric proteins that were unable to induce karmellae might simply have been present at

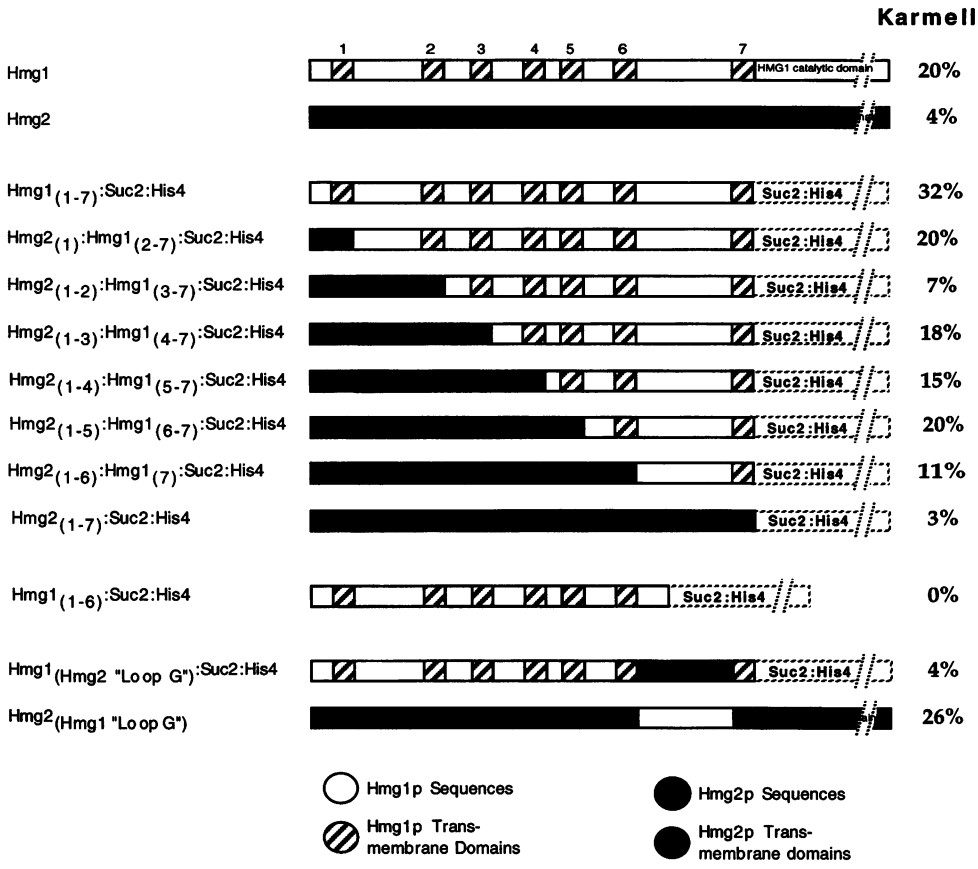

Figure 2. Summary of karmellae assembly in populations of cells expressing the chimeric Hmg1p:Hmg2p proteins. The fusion proteins used in this study are diagrammed together with the percentage of karmellae observed in yeast strains expressing each protein. The percentages reflected a cumulative score of at least 800 $DiOC_6$-stained cells, scored from at least three independent experiments.

lower amounts than chimeric proteins that induced karmellae. To examine this possibility, the relative levels of fusion proteins expressed in each strain were evaluated by immunoblots using antiserum against the *Suc2* gene product, invertase (Figure 5). Although variations in protein amount were present, these variations did not correlate with the ability of a fusion protein to induce karmellae. For example, cells expressing $Hmg2_{(1-7)}$:Suc2:His4p contained higher levels of fusion protein than $Hmg2_{(1-3)}$:$Hmg1_{(4-7)}$:Suc2:His4p, $Hmg2_{(1-4)}$:$Hmg1_{(5-7)}$:Suc2:His4p, or $Hmg2_{(1-5)}$:$Hmg1_{(6-7)}$:Suc2:His4p. However, the cells expressing $Hmg2_{(1-7)}$:Suc2:His4p assembled karmellae in only 3% of the cells, whereas the other strains assembled 15–20%. This observation indicated that the ability to induce karmellae was due to qualitative rather than quantitative differences.

Perinuclear Localization Was Insufficient to Induce Karmellae

The ability of a protein to induce karmellae might depend upon its specific localization within the cell. If so, proteins that induced karmellae would be present in a particular subcellular compartment, whereas proteins that cannot induce karmellae would be present in a different compartment. To examine this possibility, the subcellular localization of the fusion proteins was determined by immunofluorescence (Figure 6). Intact Hmg1p protein was present in the nuclear envelope, and enriched in karmellae membranes (Figure 6A). As expected, the $Hmg1_{(1-7)}$:Suc2:His4p fusion protein had a similar localization pattern as the intact Hmg1p protein, indicating that the Hmg1p membrane domain was sufficient for localization (Figure 6B). All of the other fusion proteins with chimeric Hmg2:Hmg1p membrane domains were also present in the nuclear envelope, in many cases displaying an asymmetric localization pattern like that of the intact Hmg1p protein (data not shown). For example, the $Hmg2_{(1-7)}$:Suc2:His4p fusion protein was present within the nuclear envelope (Figure 6C). In addition, rather than being uniformly present throughout the nuclear envelope, $Hmg2_{(1-7)}$:Suc2:His4p was asymmetrically localized in the nuclear envelope, producing a pattern that resembled the localization of Hmg1p. Surprisingly, Hmg2p had a different localization pattern. Instead of being localized in the nuclear envelope, Hmg2p was present in discrete patches just beneath the plasma membrane (Figure

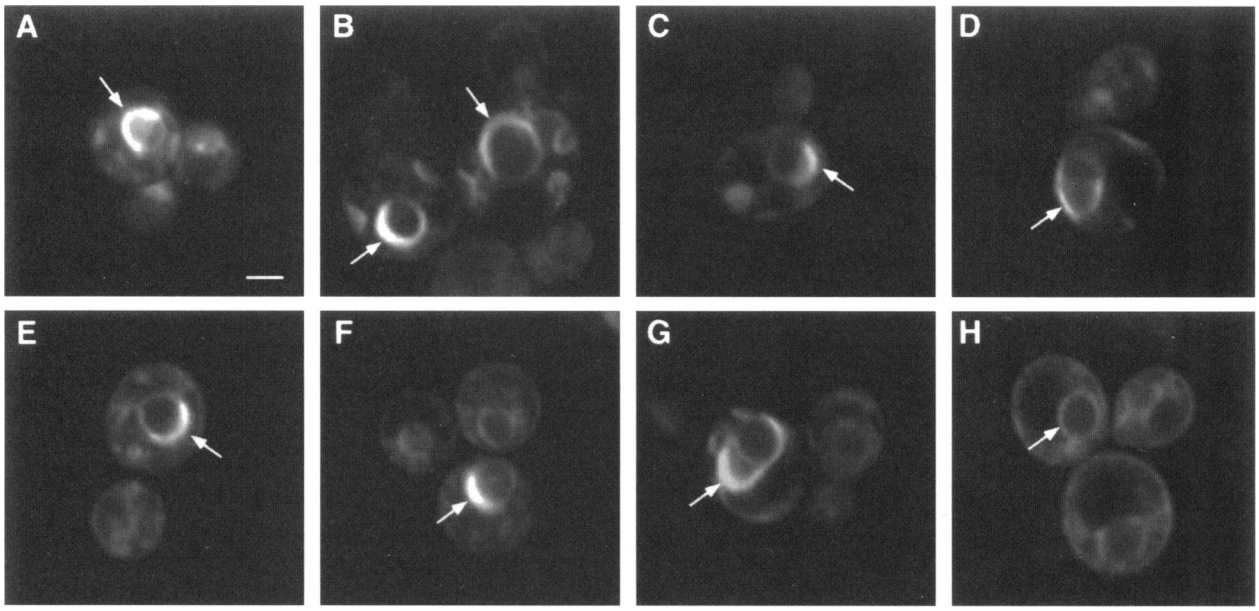

Figure 3. Analysis of exchange alleles demonstrated that transmembrane domain 7 and Loop G from Hmg1p were necessary for karmellae assembly. Confocal micrographs of $DiOC_6$-stained cells expressing the following proteins: (A) Hmg1:Suc2:His4p (JRY282), a strain expressing a fusion protein containing the entire *HMG1* membrane domain fused to *SUC2:HIS4* (karmellae present in 32% of cells); (B) $Hmg1_{(1)}$:$Hmg2_{(2-7)}$:Suc2:His4p (JRY283), a strain expressing a fusion protein containing the first transmembrane domain of *HMG2*, and the remaining membrane domain of *HMG1* fused to *SUC2:HIS4* (karmellae scored in 20% of cells); (C) $Hmg1_{(1-2)}$:$Hmg2_{(3-7)}$:Suc2:His4p (JRY284), a strain expressing a fusion protein containing the first two transmembrane domains of *HMG2*, and the remaining membrane domain of *HMG1* fused to *SUC2:HIS4* (karmellae scored in 7% of cells); (D) $Hmg1_{(1-3)}$:$Hmg2_{(4-7)}$:Suc2:His4p (JRY285), a strain expressing a fusion protein containing the first three transmembrane domains of *HMG2*, and the remaining membrane domain of *HMG1* fused to *SUC2:HIS4* (karmellae scored in 18% of cells); (E) $Hmg1_{(1-4)}$:$Hmg2_{(5-7)}$:Suc2:His4p (JRY286), a strain expressing a fusion protein containing the first four transmembrane domains of *HMG2*, and the remaining membrane domain of *HMG1* fused to *SUC2:HIS4* (karmellae scored in 15% of cells); (F) $Hmg1_{(1-5)}$:$Hmg2_{(6-7)}$:Suc2:His4p (JRY287), a strain expressing a fusion protein containing the first five transmembrane domains of *HMG2*, and the remaining membrane domain of *HMG1* fused to *SUC2:HIS4* (karmellae scored in 20% of cells); (G) $Hmg1_{(1-6)}$:$Hmg2_{(7)}$:Suc2:His4p (JRY288), a strain expressing a fusion protein containing the first six transmembrane domains of *HMG2*, and the remaining membrane domain of *HMG1* fused to *SUC2:HIS4* (karmellae scored in 11% of cells). The karmellae in this strain frequently looped away from the nucleus, as shown in this cell; (H) Hmg2:Suc2:His4p (JRY289), a strain expressing a fusion protein containing the *HMG2* membrane domain fused to *SUC2:HIS4* (karmellae scored in 3% of cells). Confocal microscopy; Bar, 2 μm.

6D). Thus, it appeared that sequences in the carboxyl terminus of Hmg2p were important for localization. Regardless of this unexpected result, the $Hmg2_{(1-7)}$:Suc2:His4p protein was present in the nuclear envelope but did not induce karmellae formation. Therefore, localization of the Hmg2p membrane domain in the same compartment as Hmg1p was not sufficient to induce karmellae.

The Loop between Transmembrane Domains 6 and 7 of Hmg1p Was Necessary and Sufficient to Induce Karmellae Assembly

The results thus far suggested that a karmellae-inducing signal was present in the Hmg1p membrane domain region that included Loop G and transmembrane domain 7. To test whether the signal might be limited to Loop G sequences, we constructed a new fusion in which the Hmg1p Loop G was replaced with the Hmg2p Loop G sequences. As expected, the $Hmg1_{(Hmg2\ Loop\ G)}$:Suc2:His4p fusion was unable to efficiently induce karmellae (Figures 2 and 7B), indicating that the Hmg1p Loop G sequences were necessary for karmellae assembly.

To test whether or not the sequences in the Hmg1p Loop G were sufficient for karmellae formation, we constructed a complementary fusion in which the Hmg1p Loop G sequences were placed into the Hmg2p context. This fusion differed from the others described in this report in that it contained the native Hmg2p catalytic domain rather than a Suc2:His4p carboxyl terminus. The Hmg2p protein with the Hmg1p Loop G efficiently assembled karmellae, indicating that Hmg1p Loop G contained sequences that were sufficient for karmellae induction, at least in the general context of an HMG-CoA reductase membrane domain (Figures 2 and 7D).

For both Loop G exchange alleles, immunoblotting experiments were used to examine the relative steady-state levels of the altered HMG-CoA reductase protein. For this analysis, $Hmg1_{(1-7)}$:Suc2:His4p levels

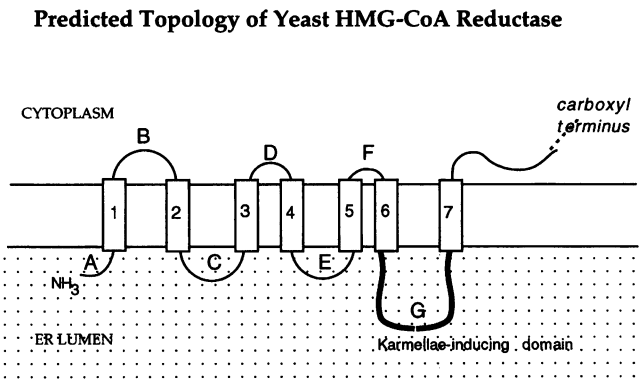

Figure 4. Diagram of the predicted topology of the karmellae-inducing region of HMG1. Current models for yeast HMG-CoA reductase topology predict seven transmembrane domains. However, experiments that test topology of mammalian HMG-CoA reductase are consistent with the presence of eight transmembrane domains (Roitelman *et al.*, 1992). The region of HMG1 that was sufficient for karmellae induction is depicted by the thicker lines.

were compared with $Hmg1_{(Hmg2\ Loop\ G)}$:Suc2:His4p using anti-invertase antiserum and Hmg2p levels were compared with $Hmg2_{(Hmg1\ Loop\ G)}$ using antiserum against the carboxyl terminal 15 amino acids of Hmg2p. In both cases, similar amounts of altered protein were produced relative to controls, ruling out the possibility that Loop G simply affected protein quantity (Figure 8).

DISCUSSION

A Membrane-inducing Signal Was Present in the Hmg1p Membrane Domain

As a step toward understanding the processes involved in membrane biogenesis, we have focused on karmellae, the specialized membrane array assembled by yeast cells in response to increases in HMG-CoA reductase levels. To identify the sequences of the Hmg1p protein that were required for karmellae biogenesis, a series of recombinant proteins was analyzed. These proteins contained chimeric membrane domains in which different amounts of the Hmg1p membrane domain, which induces karmellae, were replaced with the corresponding region of the Hmg2p membrane domain, which induces different membrane arrays.

Our analysis demonstrated that the information required for karmellae biogenesis was present within the Hmg1p Loop G sequence (Figure 4). The ability of this region to induce karmellae was assayed in the context of the normal topology of an HMG-CoA reductase membrane domain that provided the best controlled environment to test its function. In addition to Loop G, ultrastructural analysis indicated that the loop between the 5th and 6th transmembrane domains

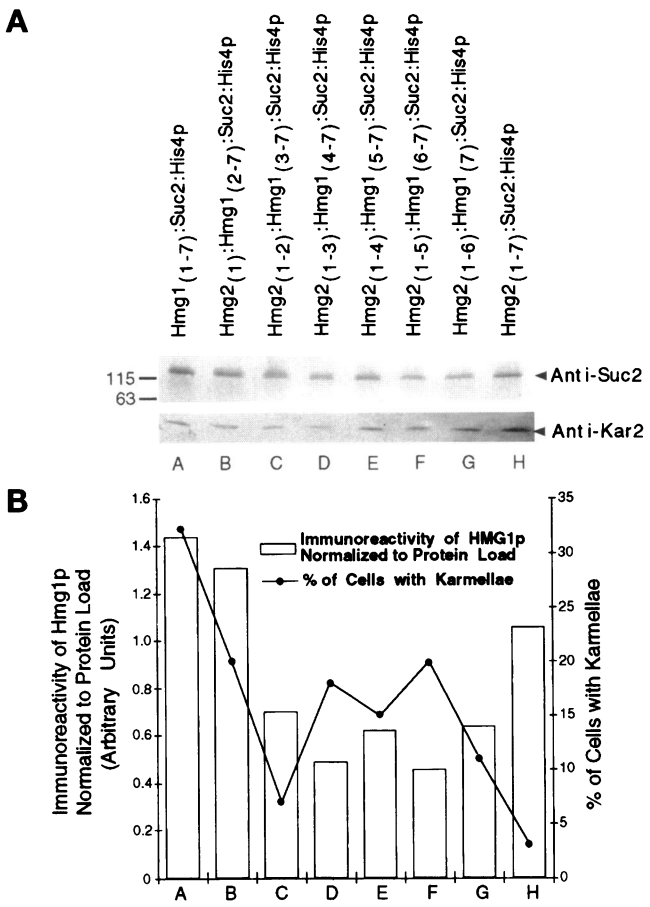

Figure 5. The abilities of different proteins to induce karmellae was unlikely to be due to quantitative differences in protein amount. (A) Immunoblot of total crude membrane preparations probed with antiserum that recognized the invertase (Suc2p) portion of the fusion protein. Note that $Hmg1_{(1-7)}$:Suc2:His4p (lane A) accumulated the greatest amount of the fusion protein and also generated karmellae in the highest proportion of cells in the population. In contrast, $Hmg2_{(1-7)}$:Suc2:His4p (lane H), which does not assemble karmellae, accumulated higher amounts of fusion protein than $Hmg2_{(1-3)}$:$Hmg2_{(4-7)}$ (lane D) or $Hmg2_{(1-4)}$:$Hmg1p_{(5-7)}$:Suc2:His4p (lane E), which assembled karmellae in 15–20% of the population. Thus, the inability of Hmg2:Suc2:His4p to induce karmellae did not reflect a decreased accumulation of the protein relative to the karmellae-inducing proteins. As a control for gel loading, the blot was also probed with antisera against the ER protein Kar2p. (B) The graph compares the fusion protein levels, normalized to total protein, and the amount of karmellae induced by each chimeric protein. There was no simple correlation between the amount of fusion protein and the capacity to induce karmellae, indicating that qualitative differences in the proteins were important determinants of karmellae-inducing ability.

("Loop E") appeared to be important for close association of the resulting membranes with the nucleus (Wright, unpublished observations). Interestingly, Loop E is predicted to be located in the cytoplasm, whereas Loop G is predicted to lie within the ER lumen (Sengstag *et al.*, 1990).

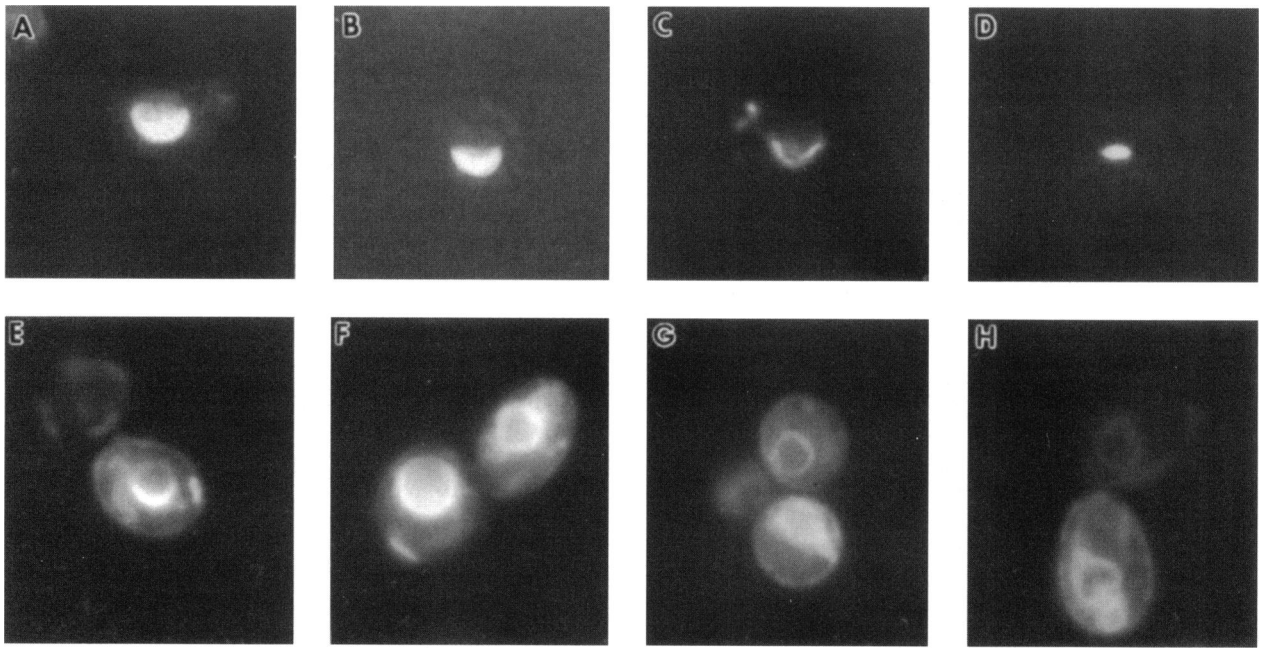

Figure 6. The Hmg2:Suc2:His4p fusion protein had an unexpected subcellular localization. (A–D) Immunofluorescence localization of HMG-CoA reductase or fusion proteins. (A) Hmg1p (JRY383), localization of intact HMG1 using affinity-purified antiserum against the HMG1 catalytic domain. HMG1 was present in the nuclear envelope, enriched in the karmellae membrane layers. (B) Hmg1:Suc2:His4p (JRY282), localization of fusion protein using affinity-purified antiserum against invertase (recognizes the Suc2p portion of the fusion protein). This fusion protein had a similar localization pattern as HMG1, asymmetrically localized within the nuclear envelope. (C) Hmg2:Suc2:His4p (JRY289), localization of fusion protein using affinity-purified antiserum against invertase (recognizes the Suc2p portion of the fusion protein). Unexpectedly, this fusion protein was not present in the same location as the intact Hmg2 protein (see panel D). Instead, in many cells, it was present in the nuclear envelope. The localization was not uniform, but also asymmetric as observed for Hmg1p and the Hmg1:Suc2:His4p fusion proteins. (D) Hmg2p (JRY249), localization of Hmg2p protein using affinity-purified antiserum against the carboxyl-terminal 15 amino acids of the catalytic domain. Hmg2p was not localized in the nuclear envelope. Instead, it was present in patches near the cell periphery. Although not obvious in this photograph, the brightly stained region was present just beneath the plasma membrane. Cells contained one or more of these Hmg2p-containing structures. (see also Figure 7C). (E–F) $DiOC_6$ staining of representative cells from the same cultures as those processed for immunofluorescence. Note that these micrographs do not correspond to the same cells shown in panels A–D. (Current immunofluorescence protocols are not compatible with retention of $DiOC_6$ staining patterns, making co-localization impossible.) (E) Hmg1p (JRY383). (F) Hmg1:Suc2:His4p (JRY282). (G) Hmg2:Suc2:His4p (JRY289). (H) Hmg2p (RWY249). Fluorescence microscopy, 1200×.

Several conclusions concerning HMG-CoA reductase-induced membrane assembly came from these data. First, fusion proteins in which the entire catalytic domain was replaced with heterologous sequences assembled karmellae. Thus, the membrane domain was both necessary and sufficient for induction of membrane biogenesis and for determining the organization of the resulting membranes. This result ruled out the possibility that membrane biogenesis in response to HMG-CoA reductase was merely due to increased sterol biosynthesis. Second, the region required for karmellae biogenesis was present in a specific, contiguous region of the membrane domain. Third, the ability to induce karmellae did not correlate with either quantitative differences between the fusion proteins nor with differences in their subcellular localization. Thus, the inability of Hmg2p to induce karmellae was not due to lower relative amounts of the protein nor to its presence in a membrane that was incapable of assembling karmellae. Taken together, our results supported the notion that induction of karmellae biogenesis involved interactions between the Hmg1p membrane domain Loop G and other cellular components.

The HMG-CoA reductase membrane domain has three known functions in mammalian cells. It is required for subcellular localization of the enzyme (Skalnik *et al.*, 1988), for control of HMG-CoA reductase half-life in response to sterols (Chin *et al.*, 1985; Gil *et al.*, 1985; Jingami *et al.*, 1987), and for induction of membrane biogenesis in response to increases in HMG-CoA reductase levels (Chin *et al.*, 1982; Skalnik *et al.*, 1985, 1988; Chun and Simoni, 1992). Specific regions of the membrane domain have been identified that are necessary for regulation of half-life in response to sterols (Jingami *et al.*, 1987; Skalnik *et al.*, 1988; Chun and Simoni, 1992). In addition, the role of certain membrane regions in induction of membrane biogenesis has been examined (Jingami *et al.*, 1987). Interestingly, an HMG-

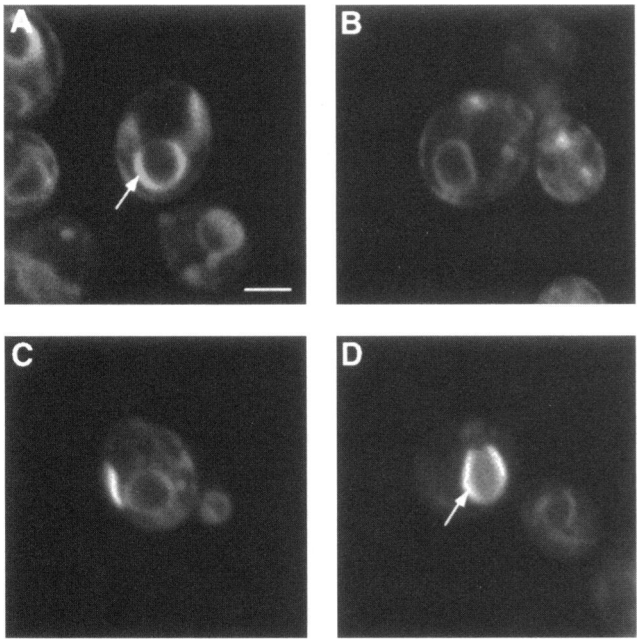

Figure 7. The ER-lumenal Loop G from Hmg1p was necessary and sufficient to induce karmellae. (A) Karmellae were present in approximately 30% of $DiOC_6$-stained cells expressing Hmg1:Suc2:His4p. (B) Replacement of the Hmg1p Loop G sequences with the corresponding Hmg2p sequences (in Hmg1:Suc2:His4p) attenuated karmellae-inducing ability to 4%. (C) Karmellae were not observed in cells expressing Hmg2p. Instead, a morphologically different proliferation of membranes was present. Frequently, one or more short strips of membrane were located near the plasma membrane of these cells, as shown in this figure. (D) Replacement of the Hmg2p Loop G sequences with the corresponding Hmg1p sequences enabled Hmg2p to induce karmellae membranes efficiently. Confocal microscopy, Bar, 2 μm.

CoA reductase allele in which the sequences encoding transmembrane domains 4 through 5 were deleted was capable of inducing membrane proliferation, but the membranes were not organized into the highly structured crystalloid ER structures induced by wild-type mammalian HMG-CoA reductase (Jingami *et al.*, 1987). The picture that is beginning to emerge indicates that the membrane domain of HMG-CoA reductase comprises a mosiac of different functions that map to discrete regions (Skalnik *et al.*, 1988; Chun *et al.*, 1990; Chun and Simoni, 1992).

Recent work has shown the membrane domain also mediates half-life control of the yeast Hmg2p (Hampton and Rine, 1994). In these studies, the sequences in Hmg2p needed for regulated degradation are present in "Loop B" (Hampton and Rine, 1994). In contrast, results presented in this paper demonstrate that the sequences of Hmg1p needed for karmellae assembly were present in Loop G. Thus, different functions of the membrane domain appear to be mediated by different regions of the membrane domain.

The amino acid sequences of the Hmg1p and Hmg2p Loop G are compared in Figure 9. Loop G, which was necessary and sufficient for induction of karmellae biogenesis, is one of the membrane domain regions with the least homology between Hmg1p and Hmg2p (Basson *et al.*, 1988). Of the 76 amino acids in this sequence, 33 are identical (43%). However, the homology is not uniformly distributed throughout the sequence. Instead, the differences cluster into certain areas (boxed in Figure 9). Based on Chou and Fasman algorithms performed by the program MacDNASIS (Hitachi Software Engineering, San Bruno, CA), the predicted secondary structures of Hmg1p and Hmg2p Loop G are also different (Figure 9). Note the helix and turn structures in the first boxed region of Hmg1p versus the predicted sheet structure for the corresponding region of Hmg2p. In addition, the predicted structure

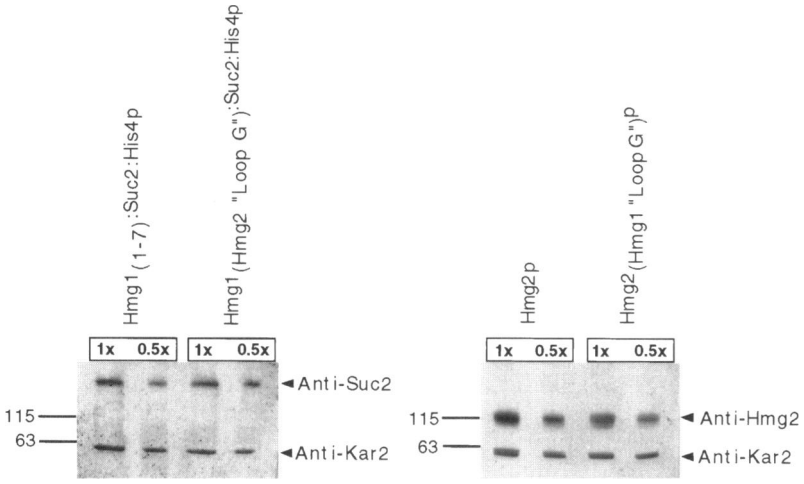

Figure 8. Exchanges of Loop G sequences did not alter relative steady-state levels of protein. (A) Immunoblot of total crude membrane preparations probed with antiserum that recognized either the invertase (Suc2p) portion of the fusion protein (blot on left) or the Hmg2p carboxyl terminus (blot on right). Similar amounts of protein were present in $Hmg1_{(1-7)}$:Suc2:His4p and $Hmg1_{(Hmg2\ Loop\ G)}$:Suc2:His4p. However, the level of $Hmg2_{(Hmg1\ Loop\ G)}$ was approximately 25% less than that of Hmg2p. Nevertheless, even though cells expressing $Hmg2_{(Hmg1\ Loop\ G)}$ contained less of the protein, they still assembled karmellae efficiently, whereas cells expressing higher levels of intact Hmg2p did not. The blots were also probed with antiserum against the ER protein Kar2p, as a control for gel loading.

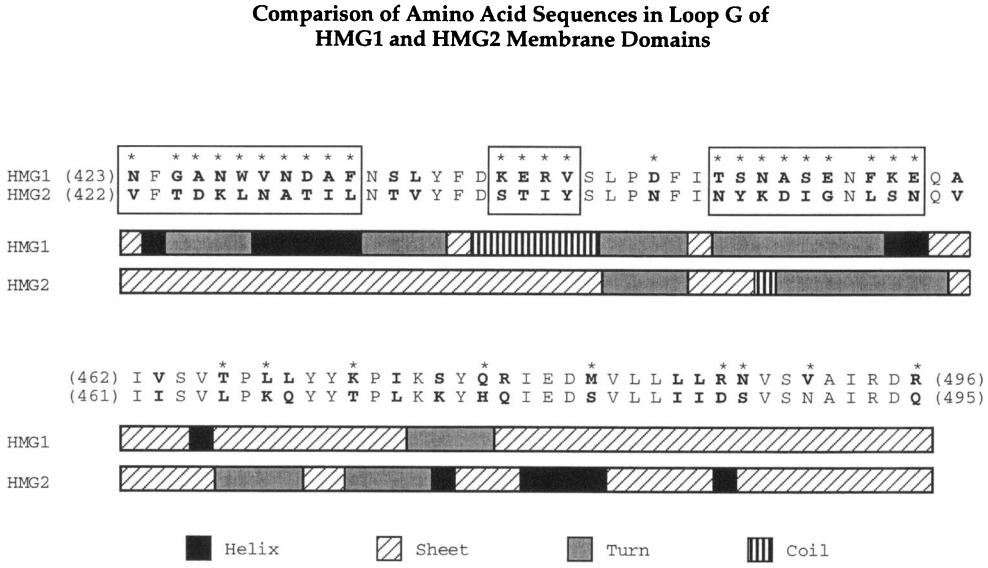

Figure 9. Comparison of the amino acid sequences and predicted secondary structures of Loop G sequences from Hmg1p and Hmg2p. Amino acid differences are marked in bold print. Nonconservative changes are marked by a star. The boxed regions are areas of high divergence. Schematic representations are based on the Chou and Fasman method of secondary protein structure prediction, performed by the MacDNAsis program. Black areas represent α-helical structure. Diagonal lines represent areas of β sheets. Gray areas represent β turn regions. Vertical line patterns represent areas of coiled structure.

of the second block of divergent amino acids of Hmg1p is a coil, whereas Hmg2p is a sheet. These structural and sequence differences are consistent with the abilities of Hmg1p and Hmg2p to induce different cellular responses.

Coupling of Membrane Assembly to Synthesis of Specific Membrane Proteins Is Not Common

Conceivably, alterations in the amount of any membrane protein could affect membrane assembly. However, surprisingly few membrane proteins have been identified that can produce readily observable alterations in membrane assembly or organization. In prokaryotes, three cases have been reported. When expressed at 25–50 times greater levels than in wild-type *Escherichia coli*, fumarate reductase (Weiner *et al.*, 1984; Elmes, 1986), ATP synthase (Von Meyenburg *et al.*, 1984), or *sn*-glycerol-3-phosphate acyltransferase (Wilkenson *et al.*, 1986, 1992) cause formation of plasma membrane invaginations that appear as tubules intruding into the cytoplasm. These membrane proliferations consist of protein/lipid crystals in which as much as 90% of the protein present within the membranes is the overproduced protein or proteins. Perhaps not surprisingly, cells containing these tubules grow very slowly, or not at all, indicating that the presence of these membranes disrupts essential cellular functions.

Alteration of membrane organization occurs in many situations in eukaryotic cells (for examples: Ghadially, 1976; Karnaky *et al.*, 1984; York and Dickson, 1985; Braunbeck *et al.*, 1987; Ho, 1987; Nott and Moore, 1987; Lopez-Iglesias and Puvion-Dutilleul, 1988; Thiaw *et al.*, 1988; Kandasamy and Kristen, 1989; Kerr and Weiss, 1991). However, as in prokaryotic cells, few specific proteins have been identified that are capable of mediating these alterations. The two best characterized examples involve the smooth ER proteins, cytochrome P450 and HMG-CoA reductase (Orrenius *et al.*, 1965; Orrenius and Ericsson, 1966; Black, 1972; Black *et al.*, 1979; Chin *et al.*, 1982; Wright and Rine, 1989). In these cases, the membranes contain the inducing protein, as well as additional proteins, while the presence of these membranes produces few, if any observable growth defects (Orrenius *et al.*, 1965; Chin *et al.*, 1982; Kochevar and Anderson, 1987). Consequently, the membrane proliferations produced in eukaryotes are more complex than the simple lipid/protein crystals observed in prokaryotic cells. In fact, secretory proteins can pass through the crystalloid ER, indicating that it can function as an intermediate of the secretory pathway (Bergman and Fusco, 1990). Taken together, these observations raise the possibility that the coupling of membrane biogenesis to a select group of proteins may reflect basic control circuits for the synthesis of specific cellular membranes. Regardless, the ability to control membrane biogenesis by selectively altering the level of a single protein provides a useful vantage point for gaining a molecular perspective on how cells regulate the synthesis and organization of specific cellular membranes.

ACKNOWLEDGMENTS

We thank Ann J. Koning for suggesting the successful strategy for obtaining the Loop G exchanges. We are also indebted to Pek Lum and Steve Castillo for their help in the preparation of the figures. This research was supported by grants from the American Cancer Society, the American Heart Association (California Division), and the National Institutes of Health (GM-45726 to R.W. and GM-35827 to J.R.), as well as a grant from the Swiss National Science Foundation (C.S.).

REFERENCES

Anderson, R.G.W., Orci, L., Brown, M.S., Segura, L.M., and Goldstein, J.L. (1983). Ultrastructural analysis of crystalloid endoplasmic reticulum in UT-1 cells and its disappearance in response to cholesterol. J. Cell Sci. *63*, 1–20.

Andreis, P.G., Cavallini, L., Mazzocchi, G., and Nussdorfer, G.G. (1990). Effects of prolonged administration of lovastatin, an inhibitor of cholesterol synthesis, on the morphology and function of rat Leydig cells. Exp. Clin. Endocrinol. *96*, 15–24.

Basson, M.E., Thorsness, M.K., Finer-Moore, J., Stroud, R., and Rine, J. (1988). Structural and functional conservation between yeast and human 3-hydroxy-3-methylglutaryl coenzyme A reductases, the rate-limiting enzyme of sterol biosynthesis. Mol. Cell. Biol. *9*, 3797–3808.

Basson, M.L., Thorsness, M.K., and Rine, J. (1986). *Saccharomyces cerevisiae* contains two functional genes encoding 3-hydroxy-3-methylglutaryl coenzyme A reductase. Proc. Natl. Acad. Sci. USA *83*, 5563–5567.

Bergman, J.E., and Fusco, P.J. (1990). The G protein of vesicular stomatitis virus has free access into and egress from the smooth endoplasmic reticulum of UT-1 cells. J. Cell Biol. *110*, 625–635.

Black, V.H. (1972). The development of smooth-surfaced endoplasmic reticulum in adrenal cortical cells of fetal guinea pigs. Am. J. Anat. *156*, 381–418.

Black, V.H., Robbins, E., McNamara, N., and Huima, T. (1979). A correlated thin-section and freeze-fracture analysis of guinea pig adrenal cortical cells. Am. J. Anat. *156*, 453–504.

Braunbeck, T., Gorgas, K., Storch, V., and Volkl, A. (1987). Ultrastructure of hepatocytes in golden ide (*Leuciscus idus melanotus* L.; Cyprinidae: Teleostei) during thermal adaptation. Anat. Embryol. *175*, 303–313.

Chin, D.J., Gil, G., Faust, J.R., Goldstein, J.L., Brown, M.S., and Luskey, K.L. (1985). Sterols accelerate degradation of HMG CoA reductase encoded by a constitutively expressed cDNA. Mol. Cell. Biol. *5*, 634–641.

Chin, D.J., Luskey, K.L., Anderson, R.G.W., Faust, J.R., Goldstein, J.L., and Brown, M.S. (1982). Appearance of crystalloid endoplasmic reticulum in compactin-resistant Chinese hamster cells with a 500-fold elevation in 3-hydroxy-3-methylglutaryl coenzyme A reductase. Proc. Natl. Acad. Sci. USA *79*, 1185–1189.

Chin, D.J., Luskey, K.L., Faust, J.R., MacDonald, R.J., Brown, M.S., and Goldstein, J.L. (1982). Molecular cloning of 3-hydroxy-3-methylglutaryl coenzyme A reductase and evidence for regulation of its mRNA in UT-1 cells. Proc. Natl. Acad. Sci. USA *79*, 7704–7708.

Chun, K.T., Bar-Nun, S., and Simoni, R.D. (1990). The regulated degradation of 3-hydroxy-3-methylglutaryl-CoA reductase requires a short-lived protein and occurs in the endoplasmic reticulum. J. Biol. Chem. *265*, 22004–22010.

Chun, K.T., and Simoni, R.D. (1992). The role of the membrane domain in the regulated degradation of 3-hydroxy-3-methylglutaryl coenzyme A reductase. J. Biol. Chem. *267*, 4236–4246.

Deschenes, R.J., and Broach, J.R. (1987). Fatty acylation is important but not essential for *Saccharomyces cerevisiae* RAS function. Mol. Cell. Biol. *7*, 2344–2351.

DeShaies, R.J., and Schekman, R. (1987). A yeast mutant defective at an early stage in import of secretory protein precursors into the endoplasmic reticulum. J. Cell Biol. *105*, 633–645.

Elmes, M.L., Scraba, D.G., and Weiner, J.H. (1986). Isolation and characterization of the tubular organelles induced by fumarate reductase overproduction in *Escherichia coli*. J. Gen. Microbiol. *132*, 1429–1439.

Ghadially, F.N. (1976). Ultrastructural Pathology of the Cell, London, UK: Buttersworth.

Gil, G., Faust, J.R., Chin, D.J., Goldstein, J.L., and Brown, M.S. (1985). Membrane-bound domain of HMG-CoA reductase is required for sterol-enhanced degradation of the enzyme. Cell *41*, 249–258.

Goldstein, J.L., and Brown, M.S. (1990). Regulation of the mevalonate pathway. Nature *343*, 425–430.

Hampton, R.Y., and Rine, J. (1994). Regulated degradation of HMG-CoA reductase, an integral membrane protein of the endoplasmic reticulum, in yeast. J. Cell Biol. *125*, 299–312.

Ho, K.L. (1987). Ultrastructure of cerebellar capillary hemangioblastoma. Acta Neuropathol. *74*, 345–353.

Jingami, H., Brown, M.S., Goldstein, J.L., Anderson, R.G.W., and Luskey, K.L. (1987). Partial deletion of membrane-bound domain of 3-hydroxy-3-methylglutaryl coenzyme A reductase eliminates sterol-enhanced degradation and prevents formation of crystalloid endoplasmic reticulum. J. Cell. Biol. *104*, 1693–1704.

Karnaky, K.J., Lau, K.R., Garretson, L.T., and Schultz, S.G. (1984). Seasonal variations in the fine structure of the *Necturus maculosus* urinary bladder epithelium: low transporters and high transporters. Am. J. Anat. *171*, 227–242.

Kandasamy, M.K., and Kristen, U. (1989). Ultrastructural responses of tobacco pollen tubes to heat shock. Protoplasma *153*, 104–110.

Kerr, J.B., and Weiss, M. (1991). Spontaneous or experimentally induced formation of a special zone in the adrenal cortex of the adult brush-tailed possum *(Trichosurus vulpecula)*. Am. J. Anat. *190*, 101–117.

Kochevar, D., and Anderson, R.G.W. (1987). Purified crystalloid endoplasmic reticulum from UT-1 cells contains multiple proteins in addition to 3-hydroxy-3-methylglutaryl coenzyme A reductase. J. Biol. Chem. *262*, 10321–10326.

Koning, A.J., Lum, P.Y., Williams, J.M., and Wright, R. (1993). $DiOC_6$ staining reveals organelle structure and dynamics in living yeast cells. Cell Motil. Cytoskeleton *25*, 111–128.

Li, A.C., Tanaka, R.D., Callaway, K., Fogelman, A.M., and Edwards, P.A. (1988). Localization of 3-hydroxy-3-methylglutaryl coenzyme A reductase and 3-hydroxy-3-methylglutaryl coenzyme A synthase in the rat liver and intestine is affected by cholestyramine and mevinolin. J. Lipid Res. *29*, 781–796.

Liscum, L., Finer-Moore, J., Stroud, R.M., Luskey, K.L., Brown, M.S., and Goldstein, J.L. (1985). Domain structure of 3-hydroxy-3-methylglutaryl coenzyme A reductase, a glycoprotein of the endoplasmic reticulum. J. Biol. Chem. *260*, 522–530.

Lopez-Iglesias, C., and Puvion-Dutilleul, F. (1988). Ultrastructural localization of glycoproteins in rabbit fibroblasts altered by Herpes simplex virus type 1 infection. Biol. Cell *62*, 47–56.

Nott, J.A., and Moore, M.N. (1987). Effects of polycyclic aromatic hydrocarbons on molluscan lysosomes and endoplasmic reticulum. Histochem. J. *19*, 357–368.

Olender, E.H., and Simoni, R.D. (1992). The intracellular targeting and membrane topology of 3-hydroxy-3-methylglutaryl-CoA reductase. J. Biol. Chem. *267*, 4223–4235.

Orrenius, S., and Ericsson, J.L.E. (1966). Enzyme-membrane relationship in phenobarbital induction of synthesis of drug-metabolizing enzyme system and proliferation of endoplasmic membranes. J. Cell Biol. *28*, 181–198.

Orrenius, S., Ericsson, J.L.E., and Ernster, L. (1965). Phenobarbital-induced synthesis of the microsomal drug-metabolizing enzyme system and its relationship to the proliferation of endoplasmic membranes. J. Cell Biol. *25*, 627–639.

Pathak, R.K., Luskey, K.L., and Anderson, R.G.W. (1986). Biogenesis of the crystalloid endoplasmic reticulum in UT-1 cells: evidence that newly formed endoplasmic reticulum emerges from the nuclear envelope. J. Cell Biol. *102*, 2158–2168.

Pringle, J.R., Preston, R.A., Adams, A.E.M., Stearns, T., Drubin, D.G., Haarer, B.K., and Jones, E.W. (1989). Fluorescence microscopy methods for yeast. Methods Cell Biol. *31*, 357–435.

Roitelman, J., Olender, E.H., Bar-Nun, S., Dunn, J.W.A., and Simoni, R.D. (1992). Immunological evidence for eight spans in the membrane domain of 3-hydroxy-3-methylglutaryl coenzyme A reductase: implications for enzyme degradation in the endoplasmic reticulum. J. Cell Biol. *5*, 959–973.

Sengstag, C., Stirling, C., Schekman, R., and Rine, J. (1990). Genetic and biochemical evaluation of eukaryotic membrane protein topology: the polytopic structure of *S. cerevisiae* HMG-CoA reductase. Mol. Cell. Biol. *10*, 672–680.

Sherman, F., Fink, G.R., and Hicks, J.B. (1986). Methods in Yeast Genetics, Cold Spring Harbor, NY: Cold Spring Harbor Laboratory Press.

Singer, I.I., Scott, S., Kazizis, D.M., and Huff, J.W. (1988). Lovastatin, an inhibitor of cholesterol synthesis, induces hydroxymethylglutaryl-coenzyme A reductase directly on membranes of expanded smooth endoplasmic reticulum in rat hepatocytes. Proc. Natl. Acad. Sci. USA *85*, 5264–5268.

Skalnik, D.G., Brown, D.A., Brown, P.C., Friedman, R.L., Hardeman, E.C., Schimke, R.T., and Simoni, R.D. (1985). Mechanisms of 3-hydroxy-3-methylglutaryl coenzyme A reductase overaccumulation in three compactin-resistant cell lines. J. Biol. Chem. *260*, 1991–1994.

Skalnik, D.G., Narita, H., Kent, C., and Simoni, R.D. (1988). The membrane domain of 3-hydroxy-3-methylglutaryl coenzyme A reductase confers endoplasmic reticulum localization and sterol-regulated degradation onto β-galactosidase. J. Biol. Chem. *263*, 6836–6841.

Thiaw, O.T., Mattei, X., and Romond, R. (1988). Process of cytoplasmic elimination during spermiogenesis in two cyprinodontidae (teleostean fishes). J. Ultrastruct. Mol. Struct. Res. *101*, 192–198.

Von Meyenburg, K., Jorgensen, B.B., and Deurs, B.V. (1984). Physiological and morphological effects of overproduction of membrane-bound ATP synthase in *E. coli K-12*. EMBO J. *3*, 1791–1797.

Weiner, J.H., Lemire, B.D., Elmes, M.L., Bradley, R.D., and Scraba, D.G. (1984). Overproduction of fumarate reductase in *Escherichia coli* induces a novel intracellular lipid-protein organelle. J. Bacteriol. *158*, 590–596.

Wilkenson, W.O., Bell, R.M., Taylor, K.A., and Costello, M.J. (1992). Structural characterization of ordered arrays of *sn*-glycerol-3-phosphate acyltransferase from *Escherichia coli*. J. Bacteriol. *174*, 6608–6616.

Wilkenson, W.O., Walsh, J.P., Corless, J.M., and Bell, R.M. (1986). Crystalline arrays of the *Escherichia coli sn*-glycerol-3-phosphate acyltransferase, an integral membrane protein. J. Biol. Chem. *261*, 9951–9958.

Wright, R., Basson, M., D'Ari, L., and Rine, J. (1988). Increased amounts of HMG-CoA reductase induce "karmellae": a proliferation of stacked membrane pairs surrounding the yeast nucleus. J. Cell Biol. *107*, 101–114.

Wright, R., Keller, G., Gould, S.J., Subramani, S., and Rine, J. (1990). Cell-type control of membrane biogenesis induced by HMG-CoA reductase overproduction. New Biol. *2*, 915–921.

Wright, R., and Rine, J. (1989). Transmission electron microscopy and immunocytochemical studies of yeast: analysis of HMG-CoA reductase overproduction by electron microscopy. Methods Cell Biol. *31*, 473–512.

York, M.A., and Dickson, D.H. (1985). Lamellar to tubular conformational changes in the endoplasmic reticulum of the retinal epithelium of the newt, *Notophthalmus viridescens*. Cell Tiss. Res. *241*, 629–637.